Computing Sacker-Sell spectra in discrete time dynamical systems

Thorsten Hüls*

Fakultät für Mathematik, Universität Bielefeld
Postfach 100131, 33501 Bielefeld, Germany
huels@math.uni-bielefeld.de

March 30, 2009

Abstract

In this paper we develop two boundary value methods for detecting Sacker-Sell spectra in discrete time dynamical systems. The algorithms are advancements of earlier methods for computing projectors of exponential dichotomies. The first method is based on the projector residual $PP - P$. If this residual is large, then the difference equation has no exponential dichotomy. A second criterion for detecting Sacker-Sell spectral intervals is the norm of end points of the solution of a specific boundary value problem. Refined error estimates for the underlying approximation process are given and the resulting algorithms are applied to an example with known continuous Sacker-Sell spectrum, as well as to the variational equation along orbits of Hénon's map.

Keywords: Sacker-Sell spectrum, Boundary value problem, Exponential dichotomy, Dichotomy projectors.

1 Introduction

For non-autonomous difference equations of the form

$$u_{n+1} = A_n u_n, \quad n \in \mathbb{Z}$$

several characterizations of spectra have been developed in the literature cf. Dieci & Van Vleck (2007) for continuous time systems. In discrete time, a generalization

*Supported by CRC 701 'Spectral Structures and Topological Methods in Mathematics'.

to non-invertible systems in given in Aulbach & Siegmund (2001). Our focus lies on the so called Sacker-Sell spectrum, which is introduced in Sacker & Sell (1978). Its construction is based on the notion of exponential dichotomies, see Appendix A. This spectrum is the set of values $\gamma > 0$, for which the scaled equation

$$u_{n+1} = \frac{1}{\gamma} A_n u_n, \quad n \in \mathbb{Z} \tag{1}$$

possesses no exponential dichotomy on $\mathbb{Z}$. The complementary set $\mathbb{R}^+ \setminus \sigma_{\mathrm{ED}}$ is called the resolvent set.

In Dieci & Van Vleck (2002) initial value methods, based on the QR-algorithm and the SVD-decomposition are applied for computing spectral intervals in continuous time.

We apply boundary value techniques for computing Sacker-Sell spectral intervals in discrete time. Two tests are proposed; the first one is based on computing the projector residual, while the second one allows, roughly speaking, to read off from the solution of the specific boundary value problem

$$u_{n+1} = \frac{1}{\gamma} A_n u_n + \delta_{n,N-1} r, \quad n = n_-, \ldots, n_+ - 1, \quad \delta \text{ Kronecker symbol} \tag{2}$$

whether γ lies in a spectral interval or in the resolvent set. Note that the boundary value approach captures in certain respects the global behavior. The solution of (2) sensitively depends on γ, whereas a change of γ leads in the QR-method to a simple shift of intervals.

The algorithms in this paper are based on a direct approach for the numerical verification of exponential dichotomies and for computing dichotomy projectors from Hüls (2008). An extension to the Sacker-Sell spectrum requires pointwise estimates for the approximation error of the solution of (2) that are stated in Section 2, particularly in case of periodic boundary conditions.

In Section 3, our algorithms for the detection of Sacker-Sell spectral intervals are introduced. In a given interval L we choose a grid L_{g} and compute for each $\gamma \in L_{\mathrm{g}}$ a quantity that indicates, whether (1) possesses an exponential dichotomy.

The basis of the first test are approximate dichotomy projectors. We prove that the projector residual $\|PP - P\|$ is exponentially small in case of an exponential dichotomy and thus, if this expression is large, then the difference equation cannot have an exponential dichotomy. Note that it is computationally expensive to find dichotomy projectors.

A second and much cheaper test is constructed as follows. Solve (2) with boundary condition

$$u_{n_-} - u_{n_+} = x,$$

where x is a fixed vector, $\|x\| = 1$, and take the norm of the end points $v_{n_\pm} := \|u_{n_-}\| + \|u_{n_+}\|$ as an indicator. If γ lies in the resolvent set, then $v_{n_\pm} = \mathcal{O}(1)$, while $v_{n_\pm}$ is expected to be large if γ is in the spectrum.

Continuous Sacker-Sell spectrum occurs, for example, if the difference equation possesses half-sided dichotomies on $\mathbb{Z}^-$ and $\mathbb{Z}^+$ that cannot be continued to an exponential dichotomy on $\mathbb{Z}$. In spectral intervals of this type, we prove that $v_{n_\pm}$ increases exponentially fast with n_+, $-n_-$, provided the trivial solution is the only bounded solution of the homogeneous equation. The latter condition is satisfied generically either by the original or by the adjoint equation. Thus exponential growth of $v_{n_\pm}$ corresponds to spectral intervals.

We apply these algorithms to a linear test example with known continuous Sacker-Sell spectrum. In Section 4, a more realistic example is considered. Spectral intervals of the variational equation along heteroclinic and homoclinic Hénon orbits are computed. For these examples, the variational equation is asymptotically constant. In the heteroclinic case, spectral intervals are caused by half-sided dichotomies that cannot be continued to $\mathbb{Z}$. The homoclinic case exhibits only point spectrum. Finally, our algorithms are applied to a variational equation, obtained from a chaotic trajectory on the Hénon attractor.

2 Error analysis for approximations of dichotomy projectors

An algorithm for computing dichotomy projectors numerically is introduced in Hüls (2008). These results are summarized in this section and refined as well as extended error estimates are developed.

Consider the linear difference equation

$$u_{n+1} = A_n u_n, \quad n \in \mathbb{Z}, \tag{3}$$

and denote by Φ its solution operator. For the forthcoming analysis, we assume that this difference equation possesses an exponential dichotomy on $\mathbb{Z}$, see Appendix A.

A1 The difference equation (3) with matrices $A_n \in \mathbb{R}^{k,k}$, having a uniformly bounded inverse, possesses an exponential dichotomy on $\mathbb{Z}$ with data $(K, \alpha_s, \alpha_u, \bar{P}^s_n, \bar{P}^u_n)$.

The computation of dichotomy projectors is based on solving inhomogeneous linear systems of the form

$$u^i_{n+1} = A_n u^i_n + \delta_{n,N-1} e_i, \quad n \in \mathbb{Z}, \quad e_i \text{ } i\text{-th unit vector.} \tag{4}$$

Using Green's function, cf. Palmer (1988), the unique bounded solution $\bar{u}_{\mathbb{Z}}$ of (4) has the explicit form

$$\bar{u}^i_n = G(n, N)e_i, \; n \in \mathbb{Z}, \quad \text{where} \quad G(n,m) = \begin{cases} \Phi(n,m)\bar{P}^s_m, & n \geq m, \\ -\Phi(n,m)\bar{P}^u_m, & n < m, \end{cases}$$

and consequently

$$\bar{P}_N^s = \left(\bar{u}_N^1, \dots \bar{u}_N^k\right). \tag{5}$$

In numerical computations, one restricts equation (4) to a finite interval $J = [n_-, n_+] \cap \mathbb{Z}$. In Hüls (2008) the following approaches are discussed:

- A boundary value ansatz

$$\begin{aligned} u_{n+1} &= A_n u_n + \delta_{n,N-1} r, \quad n = n_-, \dots, n_+ - 1, \\ b(u_{n_-}, u_{n_+}) &= 0, \end{aligned} \tag{6}$$

  with periodic or projection boundary conditions b, defined as

$$b_{\mathrm{per}}(x,y) := x - y, \tag{7}$$

$$b_{\mathrm{proj}}(x,y) := \begin{pmatrix} Y_s^T x \\ Y_u^T y \end{pmatrix}, \tag{8}$$

  where the columns of Y_s and Y_u form a basis of $\mathcal{R}(Q^u)^\perp$ and $\mathcal{R}(Q^s)^\perp$. Q^s and Q^u are two complementary projectors, having the same rank as the stable and unstable dichotomy projectors $\bar{P}_n^s$ and $\bar{P}_n^u$, respectively. Well posedness requires the angle condition

$$\measuredangle(\mathcal{R}(\bar{P}_{n_-}^s), \mathcal{R}(Q^u)) > \sigma, \quad \measuredangle(\mathcal{R}(\bar{P}_{n_+}^u), \mathcal{R}(Q^s)) > \sigma, \tag{9}$$

  with $0 < \sigma \le \frac{\pi}{2}$ for sufficiently large $-n_-$, n_+. Note that the angle between two subspaces A and B is defined as, see Golub & Van Loan (1996),

$$\measuredangle(A,B) = \theta \in \left[0, \frac{\pi}{2}\right], \quad \text{where} \quad \cos\theta = \max_{u \in A, \|u\|=1} \max_{v \in B, \|v\|=1} u^T v.$$

- Computation of the least squares solution of (4) on J.

The question, whether the numerically computed matrix P_N^s is indeed a projector can be answered by calculating $\|P_N^s P_N^s - P_N^s\|$. This projector residual is analyzed in the following proposition with subsequent results for boundary value and least squares approximations.

Proposition 1 *Let u_n^i be an approximation of $\bar{u}_n^i$ on the intervals $J = [n_-, n_+]$, such that*

$$\|u_n^i - \bar{u}_n^i\| \le C\varepsilon_n(n_\pm), \quad i \in 1, \dots, k, \quad n \in J$$

and let $P_N^s := \left(u_N^1, \dots u_N^k\right)$. Then

$$\|P_N^s P_N^s - P_N^s\| \le \tilde{C}\varepsilon_N(n_\pm),$$

with an $n_\pm$ independent constant $\tilde{C}$.

Proof: Due to (5) the estimate $\|\bar{P}^s_N - P^s_N\| \le C_1 \varepsilon_N(n_\pm)$ holds.

Let $P^s_N = \bar{P}^s_N + R$, $\|R\| \le C_1\varepsilon_N(n_\pm)$. It follows that

$$\begin{aligned} \|P^s_N P^s_N - P^s_N\| &= \|(\bar{P}^s_N + R)(\bar{P}^s_N + R) - (\bar{P}^s_N + R)\| \\ &= \|\bar{P}^s_N \bar{P}^s_N - \bar{P}^s_N + \bar{P}^s_N R + R\bar{P}^s_N + RR - R\| \\ &= \|\bar{P}^s_N R + R\bar{P}^s_N + RR - R\| \le \tilde{C}\varepsilon_N(n_\pm). \end{aligned}$$

■

On the one hand $\|P^s_N P^s_N - P^s_N\|$ is a lower bound for the approximation error, which one can compute without knowing the exact solution. One the other hand, the error may be large even if $\|P^s_N P^s_N - P^s_N\|$ is small. Error estimates are given in the forthcoming theorems.

2.1 Projection boundary conditions

Theorem 2 *Assume* ***A1*** *and let $P^{s,u}_N(n_\pm)$ be approximations on $J = [n_-, n_+]$ of the dichotomy projectors $\bar{P}^{s,u}_N$, computed using the approach* (6) *with projection boundary conditions* (8). *Further assume that the boundary operator is defined with respect to projectors Q^s, Q^u that satisfy* (9) *and*

$$\Phi(N, n_-)\mathcal{R}(Q^u) \cap \Phi(N, n_+)\mathcal{R}(Q^s) = \{0\}. \tag{10}$$

Then

$$P^{s,u}_N(n_\pm)P^{s,u}_N(n_\pm) - P^{s,u}_N(n_\pm) = 0 \tag{11}$$

and

$$\|P^{s,u}_N(n_\pm) - \bar{P}^{s,u}_N\| \le C\left(\mathrm{e}^{-(\alpha_s+\alpha_u)(N-n_-)} + \mathrm{e}^{-(\alpha_s+\alpha_u)(n_+-N)}\right).$$

Proof: Assumption (10) enables the construction of the projector $P^s_N(n_\pm)$ with range $\Phi(N, n_+)\mathcal{R}(Q^s)$ and nullspace $\Phi(N, n_-)\mathcal{R}(Q^u)$. Define $P^u_N(n_\pm) := I - P^s_N(n_\pm)$ and $P^{s,u}_n(n_\pm) := \Phi(n, N)P^{s,u}_N(n_\pm)\Phi(N, n)$ for $n \in J$, then the cocycle property (29) is satisfied.

The boundary condition (8) requires

$$u_{n_+} \in \mathcal{R}(Q^s) = \Phi(n_+, N)\Phi(N, n_+)\mathcal{R}(Q^s) = \Phi(n_+, N)\mathcal{R}(P^s_N(n_\pm)) = \mathcal{R}(P^s_{n_+}(n_\pm))$$

and similarly $u_{n_-} \in \mathcal{R}(P^u_{n_-}(n_\pm))$. The solution of the boundary value problem is given explicitly, using Green's function

$$u_n = G(n, N)r, \quad n \in J, \quad G(n, N) = \begin{cases} \Phi(n, N)P^s_N(n_\pm), & \text{for } n_+ \ge n \ge N, \\ -\Phi(n, N)P^u_N(n_\pm), & \text{for } n_- \le n < N, \end{cases}$$

in particular $u_N = P^s_N(n_\pm)r$. With $r = e_i$, $i = 1, \ldots, k$ this yields an exact projector and consequently (11) holds.

Applying (Hüls 2008, Proposition 4), we obtain the estimate

$$\|\bar{u}_N - u_N\| \le C\left(\mathrm{e}^{-(\alpha_s+\alpha_u)(N-n_-)} + \mathrm{e}^{-(\alpha_s+\alpha_u)(n_+-N)}\right),$$

and the same estimate holds, due to Proposition 1, for the approximate dichotomy projectors.

■

Note that (11) also holds, if the rank of the reference projectors Q^u and Q^s do not equal the rank of the dichotomy projectors. Since the boundary value problem considers only finite intervals, equation (11) is even satisfied, if (3) possesses no exponential dichotomy on $\mathbb{Z}$.

2.2 Periodic boundary conditions

Errors that occur when solving (6) with generalized periodic boundary conditions

$$b(u_{n_-}, u_{n_+}) = u_{n_-} - u_{n_+} - x, \quad x \in \mathbb{R}^k \text{ fixed} \tag{12}$$

are discussed in the following theorem.

Theorem 3 *Assume **A1** and denote by $\bar{u}_{\mathbb{Z}}$ the unique bounded solution of* (4).

Then the boundary value problem (6) *with boundary operator* (12) *has a unique solution u_J fulfilling for $n \in J = [n_-, n_+]$:*

$$\|\bar{u}_n - u_n\| \le C\left(\mathrm{e}^{-\alpha_u(n_+-n)} + \mathrm{e}^{-\alpha_s(n-n_-)}\right)\left(\left(\mathrm{e}^{-\alpha_u(N-n_-)} + \mathrm{e}^{-\alpha_s(n_+-N)}\right)\|r\| + \|x\|\right) \tag{13}$$

Proof: Using Green's function, the general solution of the inhomogeneous equation (6) has the form

$$u_n = G(n,N)r + \Phi(n,n_-)v_- + \Phi(n,n_+)v_+, \quad v_- \in \mathcal{R}(\bar{P}^s_{n_-}),\ v_+ \in \mathcal{R}(\bar{P}^u_{n_+}).$$

We choose v_-, v_+ such that the boundary condition is satisfied:

$$\begin{aligned} 0 = u_{n_-} - u_{n_+} - x \;&=\; G(n_-,N)r + \Phi(n_-,n_-)v_- + \Phi(n_-,n_+)v_+ \\ &\quad -G(n_+,N)r - \Phi(n_+,n_-)v_- - \Phi(n_+,n_+)v_+ - x. \end{aligned}$$

Thus

$$v_- - v_+ + \Phi(n_-,n_+)v_+ - \Phi(n_+,n_-)v_- = -G(n_-,N)r + G(n_+,N)r + x. \tag{14}$$

Since $\|\Phi(n_+,n_-)v_- + \Phi(n_-,n_+)v_+\|$ converges to 0 exponentially fast, we obtain a unique solution v_-, v_+ of (14) with

$$\begin{aligned} \|v_\pm\| \;&\le\; C\big(\|G(n_-,N)\| + \|G(n_+,N)\|\big)\|r\| + \|x\| \\ &\le\; CK\left(\mathrm{e}^{-\alpha_u(N-n_-)} + \mathrm{e}^{-\alpha_s(n_+-N)}\right)\|r\| + \|x\|. \end{aligned}$$

As a consequence it holds for $n \in J$ with a generic constant $C > 0$

$$\begin{aligned}
\|\bar{u}_n - u_n\| &= \|\Phi(n, n_+)v_+ + \Phi(n, n_-)v_-\| \\
&\leq K\mathrm{e}^{-\alpha_u(n_+-n)}\|v_+\| + K\mathrm{e}^{-\alpha_s(n-n_-)}\|v_-\| \\
&\leq C\left(\mathrm{e}^{-\alpha_u(n_+-n)} + \mathrm{e}^{-\alpha_s(n-n_-)}\right)\left(\left(\mathrm{e}^{-\alpha_u(N-n_-)} + \mathrm{e}^{-\alpha_s(n_+-N)}\right)\|r\| + \|x\|\right).
\end{aligned}$$

■

When computing dichotomy projectors, using periodic boundary conditions (7), we apply (12) with $x = 0$ and get from Proposition 1 and (13) with $n = N$

$$\begin{aligned}
\|P_N(n_\pm)P_N(n_\pm) - P_N(n_\pm)\| \leq\ & C\left(\mathrm{e}^{-\alpha_u(n_+-N)} + \mathrm{e}^{-\alpha_s(N-n_-)}\right) \\
& \cdot\left(\mathrm{e}^{-\alpha_u(N-n_-)} + \mathrm{e}^{-\alpha_s(n_+-N)}\right)\|r\|.
\end{aligned}$$

2.3 Least squares approach

We develop a pointwise estimate by combining Theorem 3 with a uniform estimate from Hüls (2008) of the least squares solution on J.

Theorem 4 *Assume* ***A1*** *and denote by* $\bar{u}_{\mathbb{Z}}$ *the unique bounded solution of* (4).
Then the least squares solution v_J *of* (6) *satisfies the following inequality:*

$$\begin{aligned}
\|\bar{u}_n - v_n\| \leq\ & C\|r\|\left(\mathrm{e}^{-\alpha_u(n_+-n)} + \mathrm{e}^{-\alpha_s(n-n_-)}\right)\cdot \\
& (n_+ - n_-)^{\frac{1}{2}}\left(\mathrm{e}^{-\alpha(N-n_-)} + \mathrm{e}^{-\alpha(n_+-N)}\right),
\end{aligned} \tag{15}$$

where $\alpha = \min\{\alpha_s, \alpha_u\}$.

Proof: From (Hüls 2008, Theorem 4.1) we obtain that equation (6) has a unique least squares solution v_J, fulfilling the error estimate

$$\sup_{n\in J}\|\bar{u}_n - v_n\| \leq C\|r\|(n_+ - n_-)^{\frac{1}{2}}\left(\mathrm{e}^{-\alpha(N-n_-)} + \mathrm{e}^{-\alpha(n_+-N)}\right). \tag{16}$$

Note that (Hüls 2008, Theorem 4.1) gives an estimate at $N = 0$ with factor $(n_+ - n_-)$ instead of $(n_+ - n_-)^{\frac{1}{2}}$. But a simple inspection of the proof leads to the improved result (16).

For getting a point-wise estimate, we consider the boundary value problem (6) with boundary operator

$$b(u_{n_-}, u_{n_+}) = u_{n_-} - u_{n_+} - x, \qquad \text{where } x = v_{n_-} - v_{n_+}.$$

By Theorem 3, this boundary value problem has a unique solution u_J that therefore coincides with the least squares solution v_J.

Thus $\|\bar{u}_n - v_n\|$ satisfies the inequality (13) with

$$\begin{aligned}
\|x\| &= \|v_{n_-} - v_{n_+}\| \leq \|v_{n_-} - \bar{u}_{n_-}\| + \|\bar{u}_{n_-}\| + \|\bar{u}_{n_+}\| + \|\bar{u}_{n_+} - v_{n_+}\| \\
&\leq C\|r\|(n_+ - n_-)^{\frac{1}{2}}\left(\mathrm{e}^{-\alpha(N-n_-)} + \mathrm{e}^{-\alpha(n_+-N)}\right) \\
&\quad + K\mathrm{e}^{-\alpha_u(N-n_-)}\|r\| + K\mathrm{e}^{-\alpha_s(n_+-N)}\|r\|.
\end{aligned}$$

This gives the estimate (15) with a generic constant $C > 0$.

■

The corresponding estimate for dichotomy projectors, computed via the least squares approach, follows from (15) with $n = N$.

3 Sacker-Sell spectrum

The Sacker-Sell spectrum, cf. Sacker & Sell (1978), Aulbach & Siegmund (2001), Dieci & Van Vleck (2007) also called dichotomy spectrum is for discrete time dynamical systems defined as

$$\sigma_{\mathrm{ED}} = \{\gamma \in \mathbb{R}^+ : (17) \text{ possesses no exponential dichotomy on } \mathbb{Z}\},$$

where

$$u_{n+1} = \frac{1}{\gamma} A_n u_n, \quad n \in \mathbb{Z}, \tag{17}$$

and the resolvent set is $\mathbb{R}^+ \setminus \sigma_{\mathrm{ED}}$. It is well known that the Sacker-Sell spectrum consists of at most k disjoint, closed intervals, where k denotes the dimension of the space, cf. Sacker & Sell (1978).

The following characterization of exponential dichotomies, see (Palmer 1988, Proposition 2.6) gives in case of half-sided dichotomies a criterion for analyzing whether γ lies in the spectrum or in the resolvent set.

Proposition 5 *The following statements are equivalent:*

- *The difference equation* (3) *possesses an exponential dichotomy on* $\mathbb{Z}$.
- (3) *has exponential dichotomies on* $\mathbb{Z}^-$ *and* $\mathbb{Z}^+$ *with projectors of equal rank, and* (3) *has no bounded, non-trivial solution on* $\mathbb{Z}$.

Denote by $\Phi(n, m)$ the solution operator of (3). Then the solution operator of the scaled equation (17) is

$$\Phi_\gamma(n, m) = \gamma^{m-n} \Phi(n, m).$$

Let L be an interval in the resolvent set, i.e. $L \cap \sigma_{\mathrm{ED}} = \emptyset$. For $\gamma \in L$ one has

$$\|\Phi_\gamma(n, m) P_m^s\| = \gamma^{m-n} \|\Phi(n, m) P_m^s\| \le K \mathrm{e}^{-\alpha_s (n-m)} \gamma^{m-n} = K \mathrm{e}^{-(\alpha_s + \ln \gamma)(n-m)},$$

and similarly, the corresponding estimate in the unstable direction follows. Thus, the scaled equation possesses in the resolvent-interval containing 1, the same dichotomy projectors as the original equation (3). Furthermore, the dichotomy projectors as well as the constant K are in a resolvent-interval independent of γ.

Example 6 *The difference equation*

$$u_{n+1} = A_n u_n, \quad \text{where } A_n = \begin{cases} A_-, & \text{for } n \le 0, \\ A_+, & \text{for } n \ge 1, \end{cases}$$

with

$$A_- = \begin{pmatrix} 1 & & \\ & 4 & \\ & & 6 \end{pmatrix} \quad \text{and} \quad A_+ = \begin{pmatrix} 2 & & \\ & 3 & \\ & & 5 \end{pmatrix} \tag{18}$$

possesses an exponential dichotomy on $\mathbb{Z}^-$ *for* $\gamma \notin \{1,4,6\}$ *and on* $\mathbb{Z}^+$ *for* $\gamma \notin \{2,3,5\}$. *Due to Proposition 5, these dichotomies cannot be extended to* $\mathbb{Z}$ *for values of* γ *from the union of intervals* $\sigma := [1,2] \cup [3,4] \cup [5,6]$.

We transform this equation into a more general form: Let S_1 *and* S_2 *be two non-singular matrices and define the difference equation*

$$u_{n+1} = A_n u_n, \quad \text{where } A_n = \begin{cases} S_1 A_- S_1^{-1}, & \text{for } n \le 0, \\ S_2 A_+ S_2^{-1}, & \text{for } n \ge 1, \end{cases} \tag{19}$$

with matrices $A_\pm$ *from* (18). *Denote by* $P_n^{-s,-u}(\gamma)$ *and* $P_n^{+s,+u}(\gamma)$ *the corresponding half-sided dichotomy projectors of the scaled equation* (17) *on* $\mathbb{Z}^-$ *and* $\mathbb{Z}^+$. *By Proposition 5, these dichotomies can be combined to a dichotomy on* $\mathbb{Z}$, *if no bounded, non-trivial solution exists. Thus*

$$\sigma_{ED} = \sigma \quad \text{if} \quad \mathcal{R}(P_0^{-u}(\gamma)) \cap \mathcal{R}(P_0^{+s}(\gamma)) = \{0\} \text{ for } \gamma \notin \sigma. \tag{20}$$

For $\gamma \in (2,3)$, *the half-sided dichotomy projectors are*

$$P_0^{-u}(\gamma) = S_1 \begin{pmatrix} 0 & & \\ & 1 & \\ & & 1 \end{pmatrix} S_1^{-1}, \quad P_0^{+s}(\gamma) = S_2 \begin{pmatrix} 1 & & \\ & 0 & \\ & & 0 \end{pmatrix} S_2^{-1}$$

and for $\gamma \in (4,5)$ *we obtain*

$$P_0^{-u}(\gamma) = S_1 \begin{pmatrix} 0 & & \\ & 0 & \\ & & 1 \end{pmatrix} S_1^{-1}, \quad P_0^{+s}(\gamma) = S_2 \begin{pmatrix} 1 & & \\ & 1 & \\ & & 0 \end{pmatrix} S_2^{-1}.$$

Thus (20) *is equivalent to non-singularity of the matrices* $\begin{pmatrix} S_1e_2 & S_1e_3 & S_2e_1 \end{pmatrix}$ *and* $\begin{pmatrix} S_1e_3 & S_2e_1 & S_2e_2 \end{pmatrix}$.

We introduce two tests for detecting Sacker-Sell spectral intervals. In a given interval L, we choose a grid L_g and compute for each $\gamma \in L_g$ a quantity that indicates whether (17) has an exponential dichotomy. The first test is based on computing dichotomy projectors, while the second and more efficient one is based on solving two boundary value problems.

3.1 Numerical detection of Sacker-Sell spectral intervals via dichotomy projectors

From Theorem 3 and 4 we know that the projector residual $\|PP - P\|$ is small, if an exponential dichotomy exists. But if this quantity is large, then the difference equation has no exponential dichotomy.

As a toy model, we choose the difference equation from Example 6. We compute for equidistantly chosen values $\gamma \in [0.01, 10]$ the dichotomy projector $P_N^s(\gamma)$ and plot $\|P_N^s(\gamma)P_N^s(\gamma) - P_N^s(\gamma)\|$. For these calculations, the periodic boundary value ansatz or alternatively the least squares approach is applied. Note that this test is not working with projection boundary conditions, since these boundary conditions always give exact projectors, cf. Theorem 2.

When discussing the costs of boundary value and least squares approach, one sees that the boundary value approach requires to solve k linear systems (6) with unit vectors as right hand side.

The least squares solution of this problem is given as $u_J = B^+R$, where $B^+ = B^T(BB^T)^{-1}$ and

$$B = \begin{pmatrix} -A_{n_-} & I & & \\ & \ddots & \ddots & \\ & & -A_{n_+-1} & I \end{pmatrix}, \quad u_J = \begin{pmatrix} u_{n_-} \\ \vdots \\ u_{n_+} \end{pmatrix}, \quad R_i = \begin{cases} 0, & i \in J,\ i \neq N-1, \\ I, & i = N-1, \end{cases}$$

cf. Hüls (2008). For the computation of the Moore-Penrose inverse, we refer to Shinozaki et al. (1972). The dichotomy projector is the N-th block component of the solution u_J. As a consequence, the Moore-Penrose inverse contains approximations of all dichotomy projectors within the finite interval. More precisely, the n-th block-row of the $(n-1)$-th block-column of B^+ is an approximation of the dichotomy projector $\bar{P}_n^s$.

We apply these techniques to the example (19) and solve (6) for $n_- = -100$, $n_+ = 100$ and $N = 0$. In Figure 1, $\|P_N^s(\gamma)P_N^s(\gamma) - P_N^s(\gamma)\|$ is plotted over γ. Since the least squares approach computes all dichotomy projectors simultaneously, we use $P_n^s(\gamma)$ for $n = -50, \dots, 50$ for our test.

As one can see, the projectors, computed via the least squares approach detect the Sacker-Sell spectral intervals more accurately than the boundary value solution. The occurrence of the plateaus in Figure 1 is a clear evidence that the difference equation has no exponential dichotomy for the corresponding γ-values. On the other hand, the computation of these projectors is quite expensive, since the computation of the Moore-Penrose inverse requires to invert the matrix BB^T. In particular for high dimensional but sparse systems, the computation of the full matrix $(BB^T)^{-1}$ is, due to memory restrictions, impossible in practice. Alternatively, one can use singular value decomposition for computing the Moore-Penrose inverse. But this approach turns out to be numerically even more expensive.

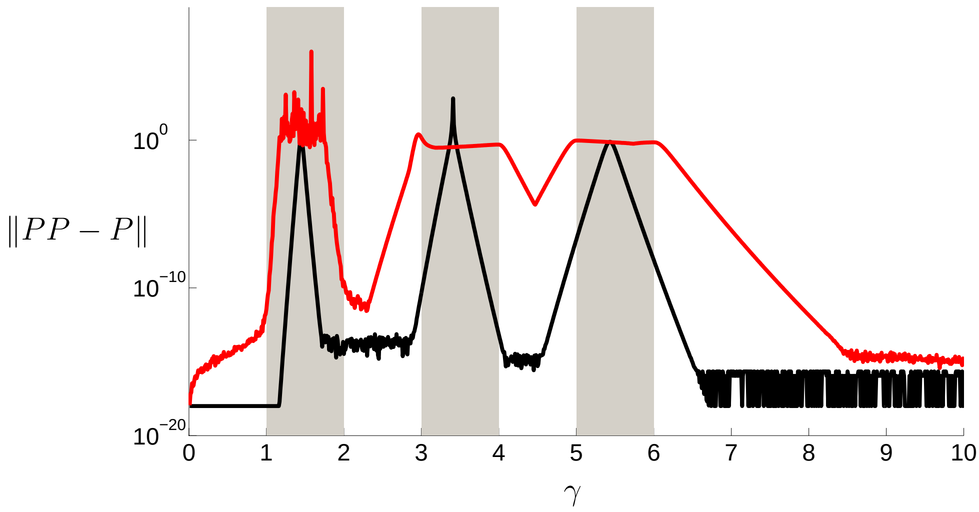

Figure 1: *Detection of Sacker-Sell spectral intervals (marked in gray) for Example 6. The red curve is computed with the least squares ansatz, while the black curve uses the boundary value approach with periodic boundary conditions.*

3.2 Numerical detection of Sacker-Sell spectral intervals via boundary value solutions

In this section, we consider Sacker-Sell spectral intervals that occur, when the difference equation has half-sided dichotomies on $\mathbb{Z}^-$ and $\mathbb{Z}^+$ with stable projectors of different rank and therefore no exponential dichotomy on $\mathbb{Z}$, see Proposition 5. We introduce a dichotomy test for this case that is based on solving boundary value problems

$$u_{n+1} = A_n u_n + \delta_{n,N-1} r, \quad n = n_-, \dots, n_+ - 1, \tag{21}$$
$$u_{n_-} = u_{n_+} + x. \tag{22}$$

Compared to the method from Section 3.1, this approach is also feasible to high dimensional systems.

Denote by $P_n^{-s,-u}$ and $P_n^{+s,+u}$ half-sided dichotomy projectors on $\mathbb{Z}^-$ and $\mathbb{Z}^+$, respectively. In the resolvent set, one has

$$\operatorname{rank}(P_N^{-u}) + \operatorname{rank}(P_N^{+s}) = k,$$

while the following cases may occur in spectral intervals:

(i) $\operatorname{rank}(P_N^{-u}) + \operatorname{rank}(P_N^{+s}) \geq k+1$. Then, the inhomogeneous equation (21) generically has infinitely many bounded solutions.

(ii) $\operatorname{rank}(P_N^{-u}) + \operatorname{rank}(P_N^{+s}) \le k-1$. In this case (21) generically has no bounded solution. Formally, we assume the generic condition (24).

The first case (i) can be reduced to (ii) by considering the adjoint equation

$$v_{n+1} = (A_{n+1}^{-1})^T v_n, \tag{23}$$

cf. Palmer (1988). If (3) possesses half-sided dichotomies with data $(K^\pm, \alpha_s^\pm, \alpha_u^\pm, P_n^{\pm s}, P_n^{\pm u})$, then the adjoint equation (23) also has half-sided dichotomies with data $(K^\pm, \alpha_u^\pm, \alpha_s^\pm, (P_{n+1}^{\pm u})^T, (P_{n+1}^{\pm s})^T)$. Obviously, the sets of γ-values coincide, in which the scaled equations

$$u_{n+1} = \frac{1}{\gamma} A_n u_n \quad \text{and} \quad v_{n+1} = \gamma (A_{n+1}^{-1})^T v_n$$

have an exponential dichotomy. If the adjoint equation has infinitely many bounded solutions on $\mathbb{Z}$, then (2) generically has no bounded solution. As a consequence, it suffices to construct a test that distinguishes (ii) from the resolvent case.

The norm of the end points u_{n_-} and u_{n_+} is an indicator for detecting spectral intervals. First, we show that in the resolvent set, this expression is bounded from above.

Assume **A1** and denote by $\bar{u}_\mathbb{Z}$ the unique bounded solution of (21) on $\mathbb{Z}$. Then Theorem 3 applies and we obtain with a generic constant $C > 0$

$$\begin{aligned}
\|u_{n_+}\| &\le \|u_{n_+} - \bar{u}_{n_+}\| + \|\bar{u}_{n_+}\| = \|u_{n_+} - \bar{u}_{n_+}\| + \|G(n_+, N) r\| \\
&\le C\left(1 + \mathrm{e}^{-\alpha_s(n_+ - n_-)}\right)\left(\left(\mathrm{e}^{-\alpha_u(N-n_-)} + \mathrm{e}^{-\alpha_s(n_+ - N)}\right)\|r\| + \|x\|\right) \\
&\quad + K\mathrm{e}^{-\alpha_s(n_+ - N)}\|r\| \\
&\le C\|x\|,
\end{aligned}$$

and similarly it holds that

$$\|u_{n_-}\| \le C\|x\|.$$

The test is based on this estimate. Roughly speaking, the difference equation (3) has no exponential dichotomy on $\mathbb{Z}$, if $\|u_{n_\pm}\|$ is noticeably larger than $\|x\|$.

An existence result for the solution of the boundary value problem as well as estimates of $\|u_{n_\pm}\|$ in case of half-sided dichotomies are given in the following theorem. Assume

$$\mathbb{R}^k = \mathcal{R}(P_N^{-u}) \oplus \mathcal{R}(P_N^{+s}) \oplus (\mathcal{R}(P_N^{-s}) \cap \mathcal{R}(P_N^{+u})) \tag{24}$$

and note that generic systems, fulfilling (ii) also satisfy this assumption.

Theorem 7 *Let $n_- < N < n_+$ and assume that 1 is not an eigenvalue of $\Phi(n_-, n_+)$.*

(i) Then the boundary value problem (21), (22) has a unique solution.

(ii) *Further assume that* (3) *possesses exponential dichotomies on* $\mathbb{Z}^-$ *and* $\mathbb{Z}^+$ *with data* $(K^\pm, \alpha_s^\pm, \alpha_u^\pm, P_n^{\pm s}, P_n^{\pm u})$*, such that*

$$\mathbb{R}^k = X \oplus Y,\ X = \mathcal{R}(P_N^{-u}) \oplus \mathcal{R}(P_N^{+s}),\ Y = \mathcal{R}(P_N^{-s}) \cap \mathcal{R}(P_N^{+u}),\ \dim Y \geq 1. \tag{25}$$

Let $r = r_X + r_Y$*,* $r_X \in X$*,* $0 \neq r_Y \in Y$*. Then*

$$\|u_{n_-}\| + \|u_{n_+}\| \geq \|r_Y\| \frac{C}{\mathrm{e}^{-\alpha_s^-(N-n_-)} + \mathrm{e}^{-\alpha_u^+(n_+-N)}}. \tag{26}$$

Proof:

(i) Two half-sided solutions of the homogeneous equation are

$$\begin{aligned} u_n^- &= \Phi(n, n_-)v_-, \quad \text{for } n \leq N, \\ u_n^+ &= \Phi(n, n_+)v_+, \quad \text{for } n \geq N. \end{aligned}$$

These half-sided solutions form a solution of the inhomogeneous equation, if

$$u_N^+ = A_{N-1}u_{N-1}^- + r \quad \Leftrightarrow \quad \Phi(N, n_+)v_+ = \Phi(N, n_-)v_- + r. \tag{27}$$

Further, the boundary condition (22) requires that $v_- = v_+ + x$.

Therefore, we get

$$\begin{aligned} \Phi(N, n_-)v_+ + \Phi(N, n_-)x + r &= \Phi(N, n_+)v_+ \\ \Leftrightarrow\ (\Phi(N, n_+) - \Phi(N, n_-))v_+ &= \Phi(N, n_-)x + r \\ \Leftrightarrow\ (\Phi(n_-, n_+) - I)v_+ &= x + \Phi(n_-, N)r. \end{aligned}$$

By assumption, $\Phi(n_+, n_-) - I$ is invertible, and we obtain a unique solution v_+, $v_- = v_+ + x$.

(ii) Let W be the projector with $\mathcal{R}(W) = Y$, $\mathcal{N}(W) = X$. Using equation (27) it follows that

$$\begin{aligned} r_Y &:= Wr = W\left(-\Phi(N, n_-)v_- + \Phi(N, n_+)v_+\right) \\ &= -WP_N^{-s}\Phi(N, n_-)v_- + WP_N^{+u}\Phi(N, n_+)v_+ \\ &= W\left(-\Phi(N, n_-)P_{n_-}^{-s}v_- + \Phi(N, n_+)P_{n_+}^{+u}v_+\right). \end{aligned}$$

From the half-sided dichotomies, we obtain

$$\begin{aligned} \|r_Y\| &\leq \|W\| \left(\|\Phi(N, n_-)P_{n_-}^{-s}\|\|v_-\| + \|\Phi(N, n_+)P_{n_+}^{+u}\|\|v_+\|\right) \\ &\leq \|W\| \left(K^-\mathrm{e}^{-\alpha_s^-(N-n_-)}\|v_-\| + K^+\mathrm{e}^{-\alpha_u^+(n_+-N)}\|v_+\|\right) \\ &\leq \tilde{C}\left(\mathrm{e}^{-\alpha_s^-(N-n_-)} + \mathrm{e}^{-\alpha_u^+(n_+-N)}\right)(\|v_-\| + \|v_+\|) \end{aligned}$$

and with $u_{n_-}^- = v_-$, $u_{n_+}^+ = v_+$ this proves (26).

■

If the difference equation possesses for all $\gamma \in \sigma^\circ_{\mathrm{ED}}$ half-sided dichotomies, then either the original or the adjoint equation generically meets assumption (25) from Theorem 7 and consequently, the corresponding solution exhibits exponential growth in the end points. This exponential growth enables the numerical detection of Sacker-Sell spectral intervals. Note that the half-sided dichotomy rates also depend on γ. At the boundary of a spectral interval α_s^- or α_u^+ is zero, while these quantities increase towards the middle of the spectral interval.

For Example 6, Figure 2 shows $\|u_{n_-}(\gamma)\| + \|u_{n_+}(\gamma)\|$ for the original and for the adjoint equation. We solve the boundary value problem for $n_- = -100$, $n_+ = 100$, $N = 0$ and for two random vectors x, r, normalized to length 1.

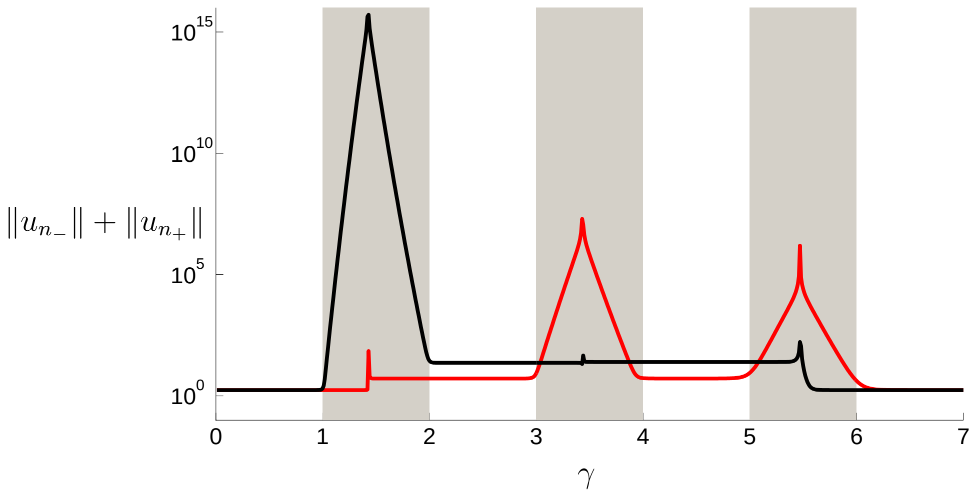

Figure 2: *Detection of Sacker-Sell spectral intervals (marked in gray) for Example 6. The black curve is computed for the original equation, while the red curve shows the result for the adjoint equation.*

4 Sacker-Sell spectrum along Hénon orbits

We apply the two algorithms from the previous section to the variational equation along orbits of the well known Hénon map, cf. Hénon (1976), Mira (1987), Devaney (1989), Hale & Koçak (1991) defined as

$$f(x) = \begin{pmatrix} 1 + x_2 - ax_1^2 \\ bx_1 \end{pmatrix} \qquad \text{with parameters} \qquad a = 1.4, \ b = 0.4.$$

4.1 Heteroclinic orbits

First, a heteroclinic orbit

$$\bar{x}_{n+1} = f(\bar{x}_n), \ n \in \mathbb{Z}, \quad \lim_{n\to\pm\infty} \bar{x}_n = \xi_\pm$$

with respect to the fixed points

$$\xi_\pm = \begin{pmatrix} z \\ bz \end{pmatrix} \quad \text{where} \quad z = \frac{b-1 \mp \sqrt{(b-1)^2+4a}}{2a}$$

is computed, using the techniques, introduced in Beyn et al. (2004), Hüls (2005).

Note that an exponential dichotomy on $\mathbb{Z}$ of the variational equation

$$u_{n+1} = Df(\bar{x}_n)u_n, \quad n \in \mathbb{Z},$$

is equivalent to transversal intersections of the unstable manifold of ξ_- with the stable manifold of ξ_+. The Sacker-Sell spectrum and especially its distance from 1 gives information about the closeness to tangential heteroclinic orbits. The results of the algorithms from the previous section are given in Figures 3 and 4.

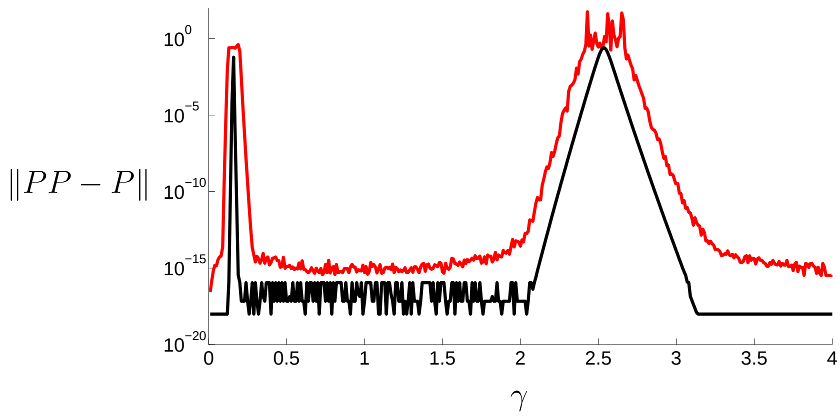

Figure 3: *Detection of Sacker-Sell spectral intervals via dichotomy projectors, for the variational equation along a heteroclinic Hénon orbit. Least squares ansatz in red and boundary value approach in black.*

Note that $Df(\xi_-)$ possesses the eigenvalues $\sigma_1 \approx -2.0376$ and $\sigma_2 \approx 0.1963$ while the eigenvalues of $Df(\xi_+)$ are $\sigma_3 \approx 3.1676$ and $\sigma_4 \approx -0.1263$. The Sacker-Sell spectrum in this example is $\sigma_{\mathrm{ED}} = [-\sigma_4, \sigma_2] \cup [-\sigma_1, \sigma_3]$.

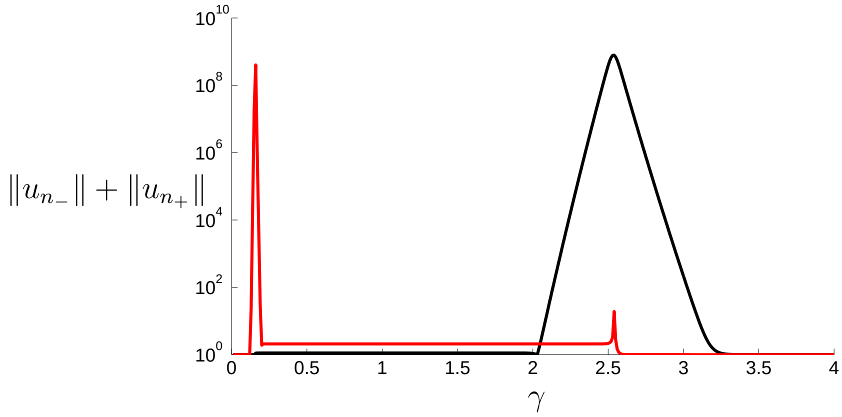

Figure 4: *Detection of Sacker-Sell spectral intervals for the variational equation along a heteroclinic Hénon orbit, via the second approach, applied to the original equation (black) and the adjoint equation (red).*

4.2 Homoclinic orbits

We apply our algorithm to the variational equation along a homoclinic orbit

$$\bar{x}_{n+1} = f(\bar{x}_n),\ \ n \in \mathbb{Z}, \qquad \lim_{n\to\pm\infty} \bar{x}_n = \xi_-.$$

In this example, the Sacker-Sell spectrum is

$$\sigma_{\mathrm{ED}} = \{-\sigma_1, \sigma_2\}.$$

Figures 5 and 6 show the resulting output of our algorithms.

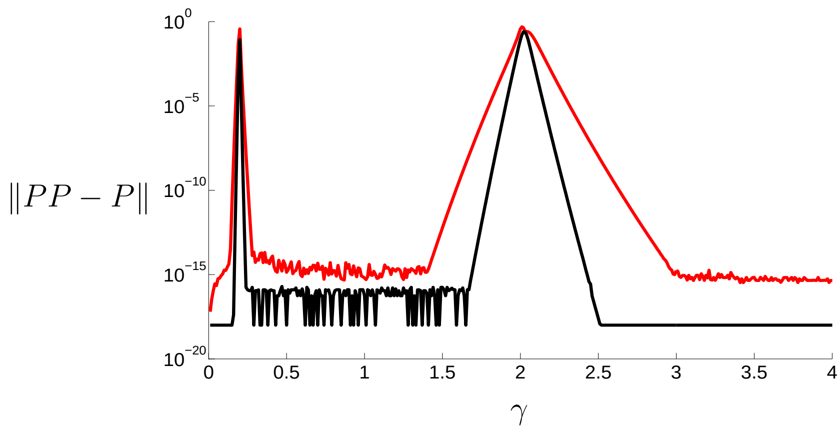

Figure 5: *Detection of Sacker-Sell spectrum via dichotomy projectors, for the variational equation along a homoclinic Hénon orbit. Least squares ansatz in red and boundary value approach in black.*

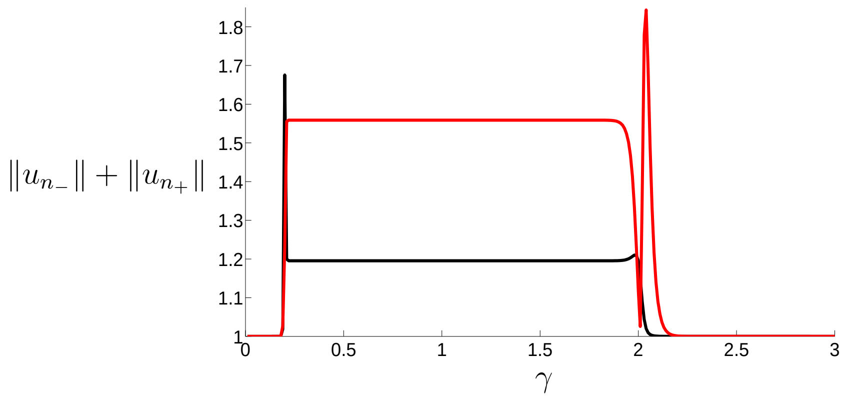

Figure 6: *Detection of Sacker-Sell spectrum for the variational equation along a homoclinic Hénon orbit, via the second approach, applied to the original equation (black) and the adjoint equation (red).*

4.3 An orbit on the attractor

We construct a chaotic orbit on the Hénon attractor for parameters $a = 1.4$, $b = 0.3$ by iterating a suitable initial point. Then our algorithms are applied to the corresponding variational equation.

In this example, the linearization is not asymptotically constant. It is not known, whether the assumptions from Section 3.2 are satisfied. Nevertheless, both approaches detect the same point spectrum, see Figures 7 and 8.

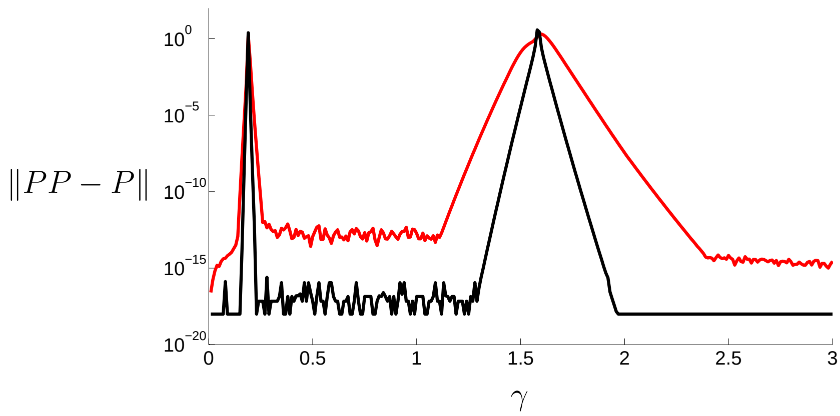

Figure 7: *Detection of Sacker-Sell spectrum via dichotomy projectors, for the variational equation along a trajectory on the attractor. Least squares ansatz in red and boundary value approach in black.*

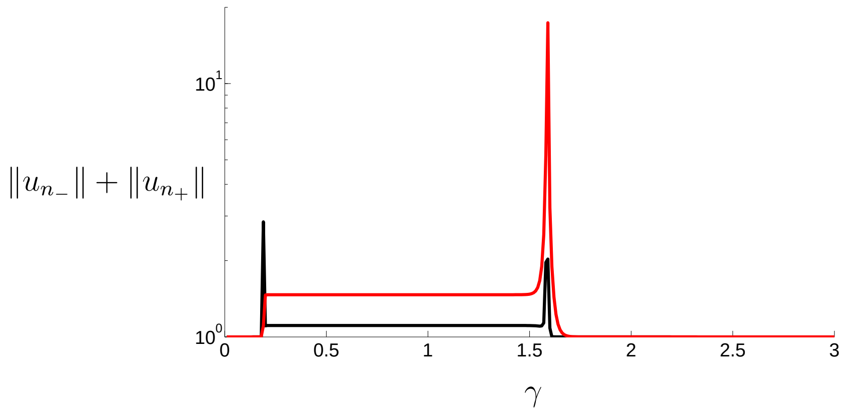

Figure 8: *Detection of Sacker-Sell spectrum for the variational equation along a trajectory on the attractor, via the second approach, applied to the original equation (black) and the adjoint equation (red).*

4.4 Conclusion

The computations indicate that the second approach via solutions of boundary value problems gives better results. It is numerically much more efficient than the computation of projector residuals, since it requires to solve for each γ only two linear inhomogeneous systems; one for the original and one for the adjoint equation. Furthermore, spectral intervals can be read off more accurately. Finally, note that Theorem 7 guarantees for the second approach in case of half-sided dichotomies exponential growth towards the middle of the spectral interval. The first approach is valuable, if additional information on the projector is needed.

A Exponential dichotomy

In this appendix, we briefly introduce the notion of an exponential dichotomy, cf. Coppel (1978), Palmer (1988). Consider the linear difference equation

$$u_{n+1} = A_n u_n, \quad n \in \mathbb{Z}, \quad A_n \text{ invertible}, \tag{28}$$

and its solution operator Φ, defined as

$$\Phi(n,m) := \begin{cases} A_{n-1} \dots A_m, & \text{for } n > m, \\ I, & \text{for } n = m, \\ A_n^{-1} \dots A_{m-1}^{-1}, & \text{for } n < m. \end{cases}$$

Definition 8 *The linear difference equation (28) possesses an* ***exponential dichotomy*** *with data $(K, \alpha_s, \alpha_u, P_n^s, P_n^u)$ on $J \subset \mathbb{Z}$, if there exist two families of projectors P_n^s and $P_n^u = I - P_n^s$ and constants $K,\ \alpha_s,\ \alpha_u > 0$, such that the following* *statements hold:*

$$P_n^s\Phi(n,m) = \Phi(n,m)P_m^s \quad \forall n,m \in J, \tag{29}$$

$$\begin{aligned} \|\Phi(n,m)P_m^s\| &\leq Ke^{-\alpha_s(n-m)} \\ \|\Phi(m,n)P_n^u\| &\leq K\mathrm{e}^{-\alpha_u(n-m)} \end{aligned} \quad \forall n \geq m,\ n,m \in J.$$

Exponential dichotomies widely apply in dynamical systems theory. For example when considering connecting orbits of fixed points or homoclinic trajectories, cf. Hüls (2007), of autonomous and non-autonomous difference equations

$$x_{n+1} = f_n(x_n), \quad n \in \mathbb{Z},$$

exponential dichotomies of the variational equation

$$u_{n+1} = Df_n(x_n)u_n, \quad n \in \mathbb{Z}$$

have a geometric interpretation. In the autonomous case stable and unstable manifolds intersect transversally cf. Palmer (1988), while in non-autonomous systems, the same holds true for the corresponding stable and unstable fiber bundles, see Hüls (2006).

Acknowledgement

The author wishes to thank Wolf-Jürgen Beyn for stimulating discussions about this paper.

References

Aulbach, B. & Siegmund, S. (2001), 'The dichotomy spectrum for noninvertible systems of linear difference equations', *J. Differ. Equations Appl.* **7**(6), 895–913. On the occasion of the 60th birthday of Calvin Ahlbrandt.

Beyn, W.-J., Hüls, T., Kleinkauf, J.-M. & Zou, Y. (2004), 'Numerical analysis of degenerate connecting orbits for maps', *Internat. J. Bifur. Chaos Appl. Sci. Engrg.* **14**(10), 3385–3407.

Coppel, W. A. (1978), *Dichotomies in Stability Theory*, Springer-Verlag, Berlin. Lecture Notes in Mathematics, Vol. 629.

Devaney, R. L. (1989), *An Introduction to Chaotic Dynamical Systems*, Addison-Wesley Studies in Nonlinearity, second edn, Addison-Wesley Publishing Company Advanced Book Program, Redwood City, CA.

Dieci, L. & Van Vleck, E. S. (2002), 'Lyapunov spectral intervals: theory and computation', *SIAM J. Numer. Anal.* **40**(2), 516–542 (electronic).

Dieci, L. & Van Vleck, E. S. (2007), ‘Lyapunov and Sacker-Sell spectral intervals’, *J. Dynam. Differential Equations* **19**(2), 265–293.

Golub, G. H. & Van Loan, C. F. (1996), *Matrix computations*, Johns Hopkins Studies in the Mathematical Sciences, third edn, Johns Hopkins University Press, Baltimore, MD.

Hale, J. K. & Koçak, H. (1991), *Dynamics and Bifurcations*, Vol. 3 of *Texts in Applied Mathematics*, Springer-Verlag, New York.

Hénon, M. (1976), ‘A two-dimensional mapping with a strange attractor’, *Comm. Math. Phys.* **50**(1), 69–77.

Hüls, T. (2005), ‘Bifurcation of connecting orbits with one nonhyperbolic fixed point for maps’, *SIAM J. Appl. Dyn. Syst.* **4**(4), 985–1007 (electronic).

Hüls, T. (2006), ‘Homoclinic orbits of non-autonomous maps and their approximation’, *J. Difference Equ. Appl.* **12**(11), 1103–1126.

Hüls, T. (2007), Homoclinic trajectories of non-autonomous maps, Technical Report 07-011, Bielefeld University, CRC 701. To appear in J. Difference Equ. Appl.

Hüls, T. (2008), Numerical computation of dichotomy rates and projectors in discrete time, Technical Report 08-081, Bielefeld University, CRC 701. To appear in Discrete Contin. Dyn. Syst. Ser. B.

Mira, C. (1987), *Chaotic dynamics*, World Scientific Publishing Co., Singapore. From the one-dimensional endomorphism to the two-dimensional diffeomorphism.

Palmer, K. J. (1988), Exponential dichotomies, the shadowing lemma and transversal homoclinic points, *in* ‘Dynamics reported, Vol. 1’, Teubner, Stuttgart, pp. 265–306.

Sacker, R. J. & Sell, G. R. (1978), ‘A spectral theory for linear differential systems’, *J. Differential Equations* **27**(3), 320–358.

Shinozaki, N., Sibuya, M. & Tanabe, K. (1972), ‘Numerical algorithms for the Moore-Penrose inverse of a matrix: direct methods’, *Ann. Inst. Statist. Math.* **24**, 193–203.